ISSN 1674-1056
http://cpb.iphy.ac.cn
http://iopscience.iop.org/cpb
中国物理 B
Chinese Physics
中国物理 Chinese Physics B

Optical investigation of topological semimetal $SrMnSb_2$

Qiu Zi-Yang(邱子阳), Liao Zhi-Yu(廖知裕), Qiu Xiang-Gang(邱祥冈)

Citation: Chin. Phys. B . 2019, 28(4): 047801. **doi:** 10.1088/1674-1056/28/4/047801
Journal homepage: http://cpb.iphy.ac.cn; http://iopscience.iop.org/cpb

What follows is a list of articles you may be interested in

Temperature-dependent Raman spectroscopic study of ferroelastic $K_2Sr(MoO_4)$

Ji Zhang(张季), De-Ming Zhang(张德明), Ran-Ran Zhang(张冉冉)
Chin. Phys. B . 2018, 27(11): 117801. **doi:** 10.1088/1674-1056/27/11/117801

Raman scattering under extreme conditions

Feng Jin(金峰), Yang Yang(杨洋), An-Min Zhang(张安民), Jian-Ting Ji(籍建葶), Qing-Ming Zhang(张清明)
Chin. Phys. B . 2018, 27(7): 077801. **doi:** 10.1088/1674-1056/27/7/077801

A general method for large-scale fabrication of Cu nanoislands/dragonfly wing SERS flexible substrates

Yuhong Wang(王玉红), Mingli Wang(王明利), Lin Shen(沈琳), Yanying Zhu(朱艳英), Xin Sun(孙鑫), Guochao Shi(史国超), Xiaona Xu(许晓娜), Ruifeng Li(李瑞峰), Wanli Ma(马万里)
Chin. Phys. B . 2018, 27(1): 017801. **doi:** 10.1088/1674-1056/27/1/017801

Different angle-resolved polarization configurations of Raman spectroscopy: A case on the basal and edge plane of two-dimensional materials

Xue-Lu Liu(刘雪璐), Xin Zhang(张昕), Miao-Ling Lin(林妙玲), Ping-Heng Tan(谭平恒)
Chin. Phys. B . 2017, 26(6): 067802. **doi:** 10.1088/1674-1056/26/6/067802

Raman scattering studies on the collapsed phase of $CaCo_2As_2$

Jianting Ji(籍建葶), Anmin Zhang(张安民), Run Yang(杨润), Yong Tian(田勇), Feng Jin(金峰), Xianggang Qiu(邱祥冈), Qingming Zhang(张清明)
Chin. Phys. B . 2016, 25(6): 067803. **doi:** 10.1088/1674-1056/25/6/067803

SPECIAL TOPIC — Topological semimetals

Optical investigation of topological semimetal $SrMnSb_2$*

Zi-Yang Qiu(邱子阳)[1,2], Zhi-Yu Liao(廖知裕)[1,2], and Xiang-Gang Qiu(邱祥冈)[1,2,3,†]

[1] *Beijing National Laboratory for Condensed Matter Physics, Institute of Physics, Chinese Academy of Sciences, Beijing* 100190, *China*
[2] *School of Physical Sciences, University of Chinese Academy of Sciences, Beijing* 100049, *China*
[3] *Collaborative Innovation Center of Quantum Matter, Beijing* 100084, *China*

(Received 23 January 2019; revised manuscript received 15 February 2019; published online 5 March 2019)

We investigate the temperature-dependent infrared spectroscopy of $SrMnSb_2$, which is a semimetal with multiple Fermi surfaces. A notable blue shift of the plasma minimum in reflectivity upon cooling indicates that the carrier density varies with temperature. In the real part of the optical conductivity $\sigma_1(\omega)$, a linearly-increased component which extrapolates to zero conductivity at finite frequency has been identified, which suggests dispersion of gapped Dirac band structures near the Fermi level. A two-Drude model, representing two different types of carriers, is introduced to describe the real part of optical conductivity. We separate the contributions of two-Drude model in dc conductivity, and demonstrate that the transport properties of $SrMnSb_2$ are mainly affected by the narrow-Drude quasiparticles. Compared with the similar phenomena observed in $CaMnSb_2$ and $SrMnBi_2$, we can infer that the two-Drude model is an appropriate approach to investigate the multiband materials in $AMnSb_2$ and $AMnBi_2$ families.

Keywords: infrared spectroscopy, topological material, Drude mode

PACS: 78.30.–j, 78.40.Kc, 78.47.–p **DOI:** 10.1088/1674-1056/28/4/047801

1. Introduction

In the past few years, a great deal of interest has been aroused in topological materials with magnetic systems that can break their time-reversal symmetry, resulting in the realization of type-II Weyl fermions.[1,2] Even though many materials are theoretically predicted as type-II Weyl semimetals, only a few have been experimentally confirmed.[3,4] Recently, AMnBi$_2$ and AMnSb$_2$ (A = Ca, Sr, Ba, Eu, and Yb) compounds have attracted much attention due to the antiferromagnetic order on Mn atoms.[5–18] Among these materials, $SrMnBi_2$, $CaMnSb_2$, and $SrMnSb_2$ share the same crystal symmetry and stacking type. Additionally, the band structures of these three materials have been calculated in detail,[8,17,19] and their electronic bands near the Fermi level are roughly identical. However, unlike the two-Drude model, which well describes the real part of optical conductivity $\sigma_1(\omega)$ of $CaMnSb_2$ and $SrMnBi_2$ at low frequency,[17,20] a single-band Drude model introduced in Ref. [21] lacks detailed fitting $\sigma_1(\omega)$ of $SrMnSb_2$. Therefore, more optical studies in the low frequency range are required for $SrMnSb_2$.

We successfully synthesize the single crystal of $SrMnSb_2$ and investigate its topological properties through infrared spectroscopy. Because of the unusual linearly dispersed band structures in topological materials, the optical conductivity of the interband transitions near the Fermi level are supposed to follow a characteristic power-law frequency dependence,

$$\sigma_1(\omega) \propto \left(\frac{\hbar\omega}{2}\right)^{d-2}, \tag{1}$$

where d is the dimension of the system.[1,22–24] Thus, when $d = 2$, $\sigma_1(\omega)$ is particularly frequency-independent, while for $d = 3$, $\sigma_1(\omega)$ should have a linearly increased range and extrapolates through the origin. In this paper, we observed a shift of the plasma minimum with varying temperature. A linearly-increased component in $\sigma_1(\omega)$ has been identified with extrapolating to zero conductivity at finite frequency, which agrees well with theoretical calculations. In the low frequency range, we introduce a two-Drude model to describe $\sigma_1(\omega)$ excellently. Therefore, the shift of the plasma minimum can be the result of a narrow Drude term which varies with temperature. The contributions of two Drude in dc conductivity have been separated, and the transport properties of $SrMnSb_2$ are mainly affected by the narrow-Drude quasiparticles. Since the two-Drude model can reasonably explain the optical and transport properties, we can infer that the two-Drude model is an appropriate approach to investigate the multiband materials in $AMnSb_2$ and $AMnBi_2$ families.

2. Experiment

The self-flux method was used to synthesize high-quality single crystals of $SrMnSb_2$.[25] The *ab*-plane reflectivity

*Project supported by the National Natural Science Foundation of China (Grant No. 11774400) and the National Key Basic Research Program of China (Grant Nos. 2015CB921102 and 2017YFA0302903).

†Corresponding author. E-mail: xgqiu@iphy.ac.cn

© 2019 Chinese Physical Society and IOP Publishing Ltd

$[R(\omega)]$ has been measured at a near-normal angle of incidence on a Bruker IFS80v spectrometer using an *in situ* gold overfilling technique.[26] Data from 50 cm^{-1} to 15000 cm^{-1} were collected at 14 different temperatures from 7 K to 295 K. $R(\omega)$ up to 30000 cm^{-1} was measured at room temperature with an Avaspec 2048 × 14 optical fiber spectrometer. Optical conductivity was calculated through Kramers–Kronig transformation of $R(\omega)$. For the low-frequency extrapolation, we used a set of Lorentz oscillators instead of the Hagen–Rubens form because of the very narrow scattering rate of the Drude component.[16,27] Above 30000 cm^{-1}, $R(\omega)$ is assumed to be constant up to 12.4 eV, above which a free-electron response (ω^{-4}) is used.

3. Results

3.1. Reflectivity

Figure 1 shows $R(\omega)$ of $SrMnSb_2$ up to 4000 cm^{-1} at all measured temperatures. The obvious peak at around 200 cm^{-1} is a response of infrared active phonon. The typical metal behavior is detected when $R(\omega)$ rapidly approaches unity, and a low-frequency sharp plasma edge shifts to higher frequency upon cooling. In addition, the minimum measured reflectance, defined as the plasma minimum, exhibits a strong temperature dependence in $R(\omega)$: as temperature is increased, the plasma minimum initially keeps constant and then red shifts, as denoted in the upper inset of Fig. 1. This change of the plasma minimum is usually associated with the temperature evolution of the carrier density.

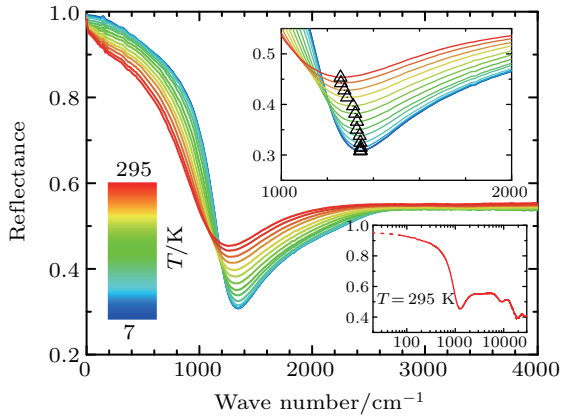


Fig. 1. Reflectivity of $SrMnSb_2$ below 4000 cm^{-1} at all measured temperatures. The upper inset denotes the evolution of plasma minima. The bottom inset shows the reflectivity up to 30000 cm^{-1} at 295 K. The red-dashed curve is the low frequency extrapolation.

3.2. Optical conductivity

Figure 2 displays $\sigma_1(\omega)$ of $SrMnSb_2$ at four represented temperatures. In the low-frequency range, $\sigma_1(\omega)$ shows obvious Drude-like response, which becomes broad when the temperature is increased. $\sigma_1(\omega)$ up to 30000 cm^{-1} is shown in the inset of bottom panel. We can infer the low carrier density from the small Drude weight compared with conventional metals.[28] Additionally, an important clue of Dirac dispersed electronic bands is that one linearly-increased optical conductivity (3000 cm^{-1}–4500 cm^{-1}) can be clearly recognized in the spectrum, alongside a sharp absorption edge from 2500 cm^{-1} to 3000 cm^{-1}. The linearly increased optical conductivity is denoted by a black dashed line in the upper inset of Fig. 2(a). The extrapolation to zero conductivity at finite frequency indicates the gapped Dirac band structure, which is consistent with the theoretical calculation in Ref. [21].

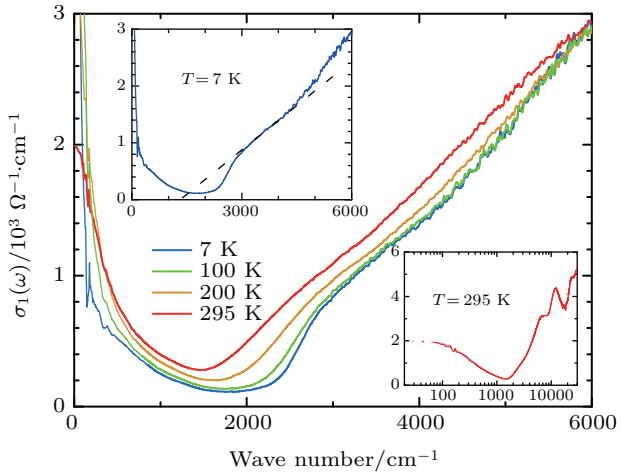


Fig. 2. The real part of optical conductivity $\sigma_1(\omega)$ of $SrMnSb_2$ at four represented temperatures. The upper inset of the panel displays the linear $\sigma_1(\omega)$ denoted with the black-dashed line. The bottom inset shows $\sigma_1(\omega)$ up to 30000 cm^{-1} at 295 K.

3.3. Low frequency fit

To quantitatively analyze the electrodynamic response, the typical Drude–Lorentz model[29] is employed to fit the low-frequency $\sigma_1(\omega)$:

$$\sigma_1(\omega) = \frac{2\pi}{Z_0}\left[\sum_k \frac{\Omega_{\mathrm{p},k}^2}{\tau_k(\omega^2+\tau_k^{-2})} + \sum_j \frac{\gamma_j\omega^2\Omega_j^2}{(\omega_j^2-\omega^2)^2+\gamma_j^2\omega^2}\right], \quad (2)$$

where $Z_0 = 377\ \Omega$ is the vacuum impedance. The first term is a sum of free-carrier Drude responses, where $\Omega_\mathrm{p} = \sqrt{4\pi ne^2/m^*}$ is the plasma frequency (n is a carrier density and m^* is an effective mass), and $1/\tau$ is the scattering rate of carriers. The second term describes a sum of Lorentz oscillators, with ω_j, γ_j, and Ω_j being the resonance frequency, linewidth and oscillator strength.

In Ref. [21], Park *et al.* suggests a single-band Drude model at low frequency. Once we have attempted to fit the measured $\sigma_1(\omega)$ with one Drude model at various temperatures, the Drude-like response narrows upon cooling, which results in the fitting at the tail of Drude response being far from satisfactory. We should know that more parameters can produce different fitting results, which would make our analysis unreliable. So in our fitting, the number of parameters is

used as little as possible to fit $\sigma_1(\omega)$ at low frequency. Therefore, a two-Drude-component model with four parameters is introduced to describe $\sigma_1(\omega)$ well at all measured temperatures, as displayed in Fig. 3(a). This two-Drude-component model coincides with the multiple Fermi surface near E_F in $SrMnSb_2$, which has been theoretically demonstrated in Ref. [19]. The interpret conductivity of the model extrapolated to zero-frequency is plotted in the inset of Fig. 3(a). The good agreement when compared to the measured dc resistivity (black solid curve) implies the fitting is reliable.

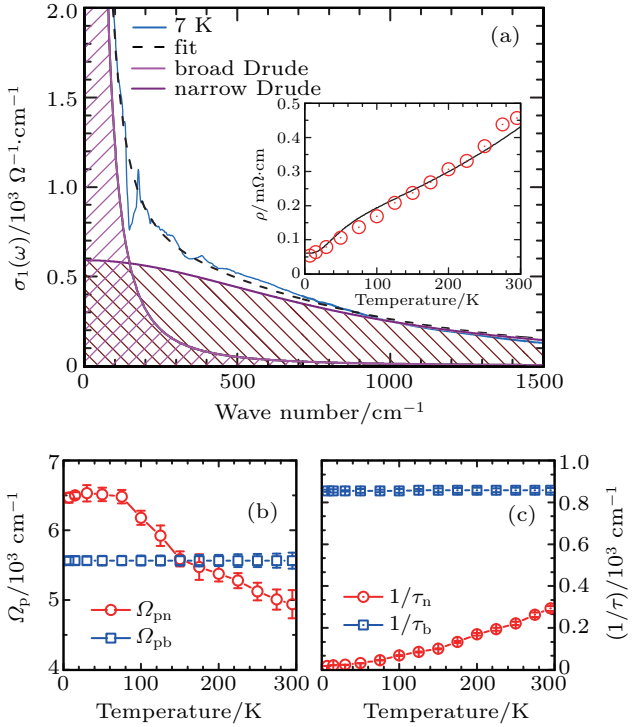


Fig. 3. (a) The blue-solid curve is the optical conductivity of $SrMnSb_2$ at 7 K in the 0 cm^{-1}–1500 cm^{-1} range. The black-dashed curve through the data is the fit which is decomposed into a narrow (magenta) and a broad (purple) Drude terms. The inset is the comparison of the measured dc resistivity (solid curve) with the inverse of the zero-frequency conductivity by fitting $\sigma_1(\omega)$ (red circles). Panels (b) and (c) portray the plasma frequency Ω_p and scattering rate $1/\tau$ for the two Drude components as a function of temperature.

The plasma frequency Ω_p and the scattering rate $1/\tau$ as a function of temperature for the two Drude components can be extracted by modeling the optical data. The temperature evolution of Ω_p, which is related to the carrier density, is traced out in Fig. 3(b). Within error bars, Ω_p's of broad Drude component (Ω_{pb}) is roughly constant, suggesting that the carrier density does not change at various temperatures, while the Ω_p's of narrow Drude component (Ω_{pn}) initially keeps constant and then increases slowly with the increasing temperature. Since Ω_{pn} changes with temperature, the spectral weight of Drude response is not constant but rather transfers to higher frequency as T is raised. Moreover, for the resembling temperature dependence of Ω_{pn}, we can infer that the T-dependent shifts in plasma minimum is solely triggered by the narrow Drude component. Figure 3(c) portrays $1/\tau$ as a function of the temperature. For narrow Drude component, $1/\tau_n$ decreases from 300 cm^{-1} to 20 cm^{-1} upon cooling, but for broad Drude, $1/\tau_b$ still exhibits no temperature dependence. The different temperature evolution of Ω_p and $1/\tau$ for the two Drude components evinces the two types of carriers in this material, which have different contributions to the transport properties of $SrMnSb_2$.

To obtain further confirmation, we extract $\sigma_1(\omega)$ at zero frequency to separate the two Drude terms' contributions to the dc conductivity in Fig. 4(a). We observed $\sigma_{1n}(0)$ decreases with increased temperature, while $\sigma_{1b}(0)$ remains constant. Since the two Drude terms affect dc conductivity through $\sigma_{total}(T) = \sigma_n(T) + \sigma_b(T)$, the fact that $\sigma_{1n}(0) > \sigma_{1b}(0)$ across all the measured temperature range indicates the quasiparticles of narrow Drude has more effect on the transport properties. Figure 4(b) portrays the two Drude corresponding resistivity yielded from the inverse of $\sigma_1(0)$. Even though $\rho_b(T)$ exhibits no temperature dependence, $\rho_n(T)$ shows a roughly identical temperature evolution to the dc resistivity in the inset of Fig. 3(a). These results demonstrate that the quasiparticles of the narrow Drude plays a major role in the transport properties.

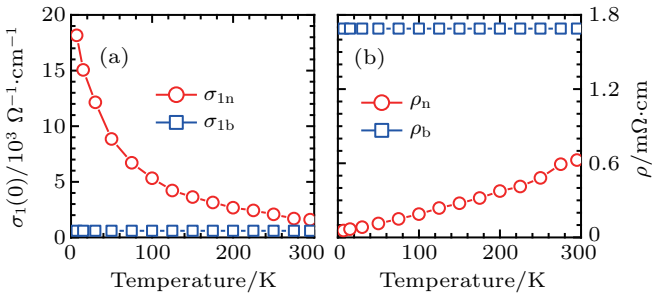


Fig. 4. (a) The contribution to dc conductivity $\sigma_1(\omega \to 0)$ at varied temperatures. (b) The corresponding resistivity through $\rho = 1/\sigma_1(\omega \to 0)$ for the narrow and broad Drude components.

Since in Ref. [30] Ling *et al.* points out that the carrier types of $SrMnSb_2$ is sensitive to the composition and growth details, it is reasonable for us to only consider the carriers' different contributions to the conductivity, and separate them into two Drude quasi-particles with different temperature dependence instead of hole or electron carriers. The carriers of broad Drude with constant scattering rate and plasma frequency at all measured temperature can produces an incoherent contribution to the conductivity, while the carriers of narrow Drude component plays a major role in dc conductivity and can explain the optical data well in our measurement. Therefore, the two different types of carriers belong to the different contributions to the conductivity.

4. Conclusion

To summarize, the detailed optical properties of $SrMnSb_2$ have been measured from 7 K to 295 K. We observe the plasma minimum initially keeps constant and then red shifts with the

increasing temperature in reflectivity, which infers that the carrier density varies with temperature. One linearly-increased component in optical spectrum has been recognized as the characteristic hallmark of a three-dimensional Dirac dispersed band structure. The finite intercept obtained through extrapolating the linear component to zero frequency indicates the gapped nature in Dirac bands, which coincides with theoretical calculations. The low-frequency optical conductivity is well-described by the superposition of two Drude components, suggesting the multiple Fermi surfaces in this material. We extract the plasma frequency and scattering rate for the two Drude terms as a function of temperature by fitting the optical data. Since the similar temperature evolution of plasma frequency observed for narrow Drude term, the T-dependent shifts of plasma minimum can be explained-well by the narrow Drude component. In addition, the contribution of the two group carriers to the dc conductivity has been traced out, and the narrow Drude subsystem plays a major role in the transport properties. Compared with the similar response detected in $CaMnSb_2$ and $SrMnBi_2$, all of these reasonable conclusions and results indicate that the two-Drude model is an appropriate approach to investigate the multiband material in $AMnSb_2$ and $AMnBi_2$ families.

Acknowledgments

We thank Wei Zhang for our useful discussions.

References

[1] Armitage N P, Mele E J and Vishwanath A 2018 *Rev. Mod. Phys.* **90** 015001
[2] Bansil A, Lin H and Das T 2016 *Rev. Mod. Phys.* **88** 021004
[3] Coulter J, Sundararaman R and Narang P 2018 *Phys. Rev. B* **98** 115130
[4] Xu N, Wang ZW, Magrez A, Bugnon P, Berger H, Matt C E, Strocov V N, Plumb N C, Radovic M and Pomjakushina E 2018 *Phys. Rev. Lett.* **121** 136401
[5] Guo Y F, Princep A J, Zhang X, Manuel P, Khalyavin D, Mazin I I, Shi Y G, Boothroyd and A T 2014 *Phys. Rev. B* **90** 075120
[6] Wan X, Turner A M, Vishwanath A and Savrasov S Y 2011 *Phys. Rev. B* **83** 205101
[7] Lee G, Farhan M A, Kim J S and Shim J H 2013 *Phys. Rev. B* **87** 245104
[8] Park J, Lee G, Wolff-Fabris F, Koh Y Y, Eom M J, Kim Y K, Farhan M A, Jo Y J, Kim C and Shim J H 2011 *Phys. Rev. Lett.* **107** 126402
[9] Wang K, Graf D, Wang L, Lei H, Tozer S W and Petrovic C 2012 *Phys. Rev. B* **85** 041101
[10] Li L, Wang K, Graf D, Wang L, Wang A and Petrovic C 2016 *Phys. Rev. B* **93** 115141
[11] Wang A, Zaliznyak I, Ren W, Wu L, Graf D, Garlea V O, Warren J B, Bozin E, Zhu Y and Petrovic C 2016 *Phys. Rev. B* **94** 165161
[12] Wang K, Graf D, Lei H, Tozer S W and Petrovic C 2011 *Phys. Rev. B* **84** 220401
[13] May A F, McGuire M A, Sales and B C 2014 *Phys. Rev. B* **90** 075109
[14] Chinotti M, Pal A, Ren W J, Petrovic C and Degiorgi L 2016 *Phys. Rev. B* **94** 245101
[15] Liu J, Hu J, Cao H, *et al.* 2016 *Sci. Rep.* **6** 30525
[16] Chaudhuri D, Cheng B, Yaresko A, Gibson Q D, Cava R J and Armitage N P 2017 *Phys. Rev. B* **96** 075151
[17] Qiu Z Y, Le C C, Dai Y M, Xu B, He J B, Yang R, Chen G F, Hu J P and Qiu X G 2018 *Phys. Rev. B* **98** 115151
[18] Wang Y Y, Xu S, Sun L L and Xia T L 2018 *Phys. Rev. Materials* **2** 021201
[19] Farhan M A, Lee G and Shim J H 2014 *J. Phys.: Condens. Matter* **26** 042201
[20] Park H J, Park B C, Lee M C, Jeong D W, Park J, Kim J S, Ji H S, Shim J H, Kim K W, Moon S J 2017 *Phys. Rev. B* **96** 155139
[21] Park H J, Sandilands L J, You J S, Ji H S, Sohn C H, Han J W, Moon S J, Kim K W, Shim J H and Kim J S 2016 *Phys. Rev. B* **93** 205122
[22] Carbotte J P 2017 *J. Phys.: Condens. Matter* **29** 045301
[23] Hosur P, Parameswaran S A and Vishwanath A 2012 *Phys. Rev. Lett.* **108** 046602
[24] Ashby P E C and Carbotte J P 2014 *Phys. Rev. B* **89** 245121
[25] He J B, Fu Y, Zhao L X, Liang H, Chen D, Leng Y M, Wang X M, Li J, Zhang S and Xue M Q 2017 *Phys. Rev. B* **95** 045128
[26] Homes C C, Reedyk M, Cradles D A and Timusk T 1993 *Appl. Opt.* **32** 2976
[27] Schilling M B, Löhle A, Neubauer D, Shekhar C, Felser C, Dressel M and Pronin A V 2017 *Phys. Rev. B* **95** 155201
[28] Beach R T and Christy R W 1997 *Phys. Rev. B* **16** 5277
[29] Dai Y M, Akrap A, Schneeloch J, Zhong R D, Liu T S, Gu G D, Li Q and Homes C C 2014 *Phys. Rev. B* **90** 121114
[30] Ling J W, Liu Y W, Jin Z, Huang S, Wang W Y, Zhang C, Yuan X, Liu S S, Zhang E Z, Huang C, Sankar R, Chou F C, Xia Z C and Xiu F X 2018 *Chin. Phys. B* **27** 017504